

CFD Simulation of Geared Transmissions with Injection Lubrication

H. Liu, F. Link, T. Lohner, K. Stahl

Introduction

Sufficient lubricant supply to all machine elements in geared transmissions is required for reliable operation. Depending on the speed, usually a small amount of lubricant is sufficient for lubricant film formation, whereas most of the lubricant is needed for cooling. As lubricant is kept in motion, lubrication always involves hydraulic losses. For oil lubrication at high speeds, the hydraulic losses can share a remarkable amount of the overall power losses of geared transmissions. Injection lubrication is a common way of lubrication particularly in high-speed transmissions, which currently attracts high attention in terms of e-mobility applications. Injection lubrication usually involves far less hydraulic power losses compared to dip lubrication and allows direct oil supply to individual machine elements as well as effective cooling and filtration by external oil supply units.

In general, no-load gear losses and oil distribution can be observed by experimental setups. Through the years, several experimental studies on injection-lubricated gears were conducted (Refs. 20–22). The observed relations on the no-load loss with regard to the gear geometry, injection volume and injection speed were partially converted into empirical equations.

According to Mauz (Ref. 21), the no-load power loss of injection-lubricated gears can be categorized as impulse, squeezing and windage power loss:

$$P_{LG0} = P_{LG0,I} + P_{LG0,S} + P_{LG0,W} \quad (1)$$

The impulse power loss $P_{LG0,I}$ occurs when injected oil impinges on the tooth flanks of the gears. Based on Aiura et al. (Ref. 4), Mauz (Ref. 21) derived a simplified approach for the impulse loss torque $T_{LG0,I}$ for gear pairs with a circumferential speed of $v_t < 60$ m/s:

$$T_{LG0,I} = C_1 \cdot r_w \cdot \rho \cdot \dot{V}_{in} \cdot (v_t \pm v_{in}) \quad (2)$$

C_1	variant coefficient	-
ρ	density	kg/m ³
v_t	circumferential speed	m/s
r_w	pitch radius	mm
\dot{V}_{in}	oil injection volume rate	l/min
v_{in}	injection speed	m/s

Note that the impulse power loss can take negative values in case of a larger injection speed than circumferential speed.

The squeezing power loss $P_{LG0,S}$ occurs when oil is squeezed out of the gear meshing zone in both axial and radial direction. Mauz (Ref. 21) derived an equation for the squeezing loss torque $T_{LG0,S}$ for gear pairs with a circumferential speed of $v_t < 60$ m/s:

$$T_{LG0,S} = C_1 \cdot 4.12 \cdot \rho \cdot r_w \cdot \dot{V}_{in}^{0.75} v_t^{1.25} b^{0.25} \cdot m_n^{0.25} \left(\frac{v}{v_0}\right)^{0.25} \cdot \left(\frac{h_z}{h_{z0}}\right)^{0.5} \quad (3)$$

C_1	variant coefficient	-
r_w	pitch radius	mm
v_t	circumferential speed	m/s
b	tooth width	mm
ν	kinematic viscosity	mm ² /s
h_z	tooth height	mm
ρ	density	kg/m ³
\dot{V}_{in}	oil injection volume rate	l/min
v_{in}	injection speed	m/s
m_n	normal module	mm
ν_0	reference viscosity	mm ² /s
h_{z0}	reference tooth height	mm

Note that the squeezing power loss is neglected if the injection speed is opposite the direction of the circumferential speed (Ref. 21).

The windage power loss $P_{LG0,W}$ is caused by a secondary medium — mostly air. For low circumferential speeds, the windage power loss shares a marginal percentage in comparison to the impulse and squeezing power loss.

The empirical equations of Mauz (Ref. 21) are easily applicable, which made them part of modern gear calculation programs for geared transmissions (e.g., Ref. 11). However, its range of application and transferability to industrial operating conditions is usually limited and many mechanisms are simplified.

Literature Review

The application of CFD (computational fluid dynamics) methods to geared transmissions provides more detailed insights into the oil flow and no-load losses (Ref. 8). CFD methods are flexible and easily applicable, have no limitations with regard to gear geometry and housing shape and can describe physical phenomena very accurately (Refs. 18–19).

Many CFD studies of geared transmissions have focused on dip lubrication. Thereby, besides finite volume (FV)-based methods, smoothed particle hydrodynamics (SPH) methods are also used. An overview of literature was given by the authors in (Refs. 17–19). Selected studies are summarized in the following.

Concli et al. (Refs. 5–7, 13) carried out many numerical studies on the oil flow and churning loss of dip-lubricated spur and planetary gears by using the FV-based CFD method. The results with respect to the gear churning loss are in good agreement with the experimental measurements. In addition to that, a specific mesh-handling technique was introduced, which is specially designed for gear meshing problems

allowing a reduction of the computing time by over 90% (Ref. 7).

Liu et al. (Refs. 18–19) applied a three-dimensional FV-based CFD model to investigate the oil flow and the churning power loss of a dip-lubricated single-stage spur gearbox. The results for both oil distribution and churning loss torque agree very well with both high-speed camera recordings and loss torque measurements. The studies show that the FV method is very suitable for predicting the oil flow and the no-load loss in geared transmissions.

Besides FV-based CFD methods, particle-based CFD methods, i.e.—smoothed particle hydrodynamics (SPH)—have been applied to geared transmissions. SPH is a Lagrangian and mesh-free method in which the medium is represented by discrete fluid elements, the motion in space and time of which is calculated through a set of equations developed by Monaghan (Ref. 23). In comparison to conventional CFD methods, SPH can easily handle free surface flows without much modeling effort due to its mesh-free nature.

Emmer (Ref. 9) was one of the first people to explore the potential of SPH for the simulation of oil flow in gearboxes. He investigated the oil flow as well as the churning losses of a dip-lubricated single gear and gear pair. The findings show that the application of SPH to gearboxes requires fundamental optimization to obtain physically plausible results on the oil flow and churning losses.

Liu et al. (Ref. 17) set up a SPH-based simulation model to investigate the oil flow and the churning loss of a dip-lubricated spur gear pair in a test gearbox. The model was studied by varying the gear speed, lubricant viscosity and oil sump temperature. The authors point out that, besides the great potential of SPH further optimizations on current SPH, codes are required for good predictions of oil flow and no-load gear loss in geared transmissions.

As indicated above, many CFD studies on dip-lubricated geared transmissions have been performed. However, there are very few numerical studies on injection lubrication.

Arisawa et al. (Refs. 1–3) investigated the impulse and windage loss of an injection-lubricated bevel gear pair for an aircraft by CFD simulation and loss measurements. They set up a three-dimensional, two-phase FV-based CFD model with a so-called porous body approach to illustrate the gear meshing. The focus of the study was the influence of the shroud of bevel gears on the no-load gear loss. The results show that the CFD simulations are quantitatively in good agreement with the measurements. It was found that the gear impulse loss takes the greatest part of the no-load gear losses, whereas the windage loss only shares a very small percentage. It was revealed that, by introducing shrouds, the no-load gear loss could be reduced by up to 36% compared to unshrouded gears. The authors also point out that by observing the oil flow by CFD, it was possible to design spur gear trains of the gearbox in a manner that prevents stagnation of oil inside the gearbox when the aircraft changes attitude.

Fondelli et al. (Ref. 10) studied the impulse loss of a single high-speed spur gear pair with injection lubrication numerically. They applied an FV-based CFD model with a local mesh refinement feature. This meshing technique allowed acceptable computing time. The simulation model captured the oil set into motion as well as the droplet and ligament formation by the breakup of the jet. It was shown that the pressure distribution on the teeth flank resulting from the oil jet impact contributes significantly to the resistance torque. The influence of the shear forces was

evaluated as negligible.

The brief literature review shows that many CFD studies have analyzed the oil flow and no-load loss of dip-lubricated geared transmissions. Only very few numerical studies have focused on injection lubrication. Within the framework of this paper, an FV-based CFD model of a single-stage injection-lubricated test gearbox of the FZG gear test rig was built to investigate the influence of the injection volume, oil viscosity and gear speed on the oil supply and distribution. The results also include a comparison of the simulated no-load gear losses with empirical calculations.

Object of Investigation and Operating Conditions

The object of investigation is the FZG no-load power loss test rig. It features the same test gearbox geometry as the test rigs used by the authors in (Refs. 17–19). The FZG no-load power loss test rig was specifically designed for experimental investigations on the oil flow and no-load loss of gears.

FZG no-load power loss test rig. The mechanical layout of the FZG no-load power loss test rig is shown (Fig. 1, left). It consists of four main parts: the electric engine, the intermediate gearbox, the loss torque meter and the test gearbox. The test gearbox is planned to be adapted for injection lubrication similar to the manner shown (Fig. 1, right).

The test rig has already been described (Ref. 18). The main parts are repeated below. The speed of the electric engine is transmitted through the intermediate gearbox and the pinion shaft to the test gearbox. The no-load loss caused

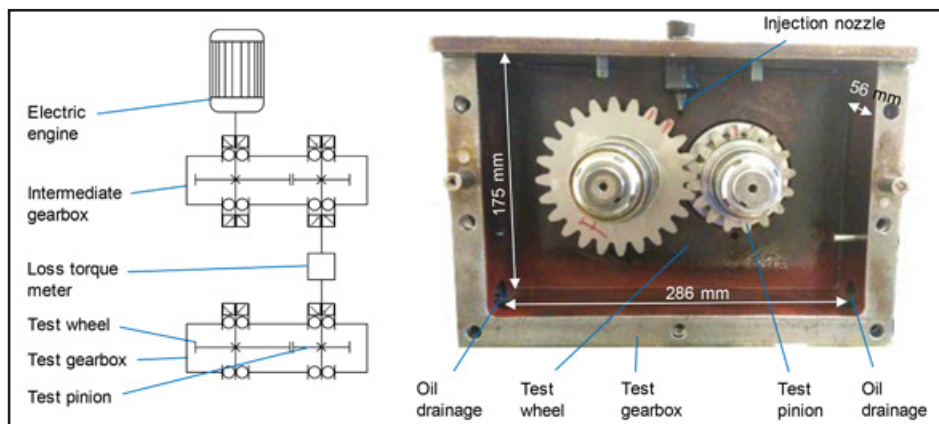


Figure 1 Mechanical layout of the FZG no-load power loss gear test rig (left); injection-lubricated test gearbox (right).

by the test gearbox is measured by the loss torque meter on the pinion shaft and includes the gear losses as well as the losses of the four bearings and two seals. In order to minimize the losses from bearings and to obtain a clear view of the oil flow from the front, small needle bearings are installed. The front cover was made of transparent acrylic glass in order to obtain a clear view of the oil flow. The considered torque meter has a measuring range of 10 Nm and a measuring error of ±0.1%.

The injection lubrication of the test gearbox is planned to be adopted from other FZG gear test rigs (Figure 1, right). The injection nozzle is placed just above the gear meshing zone. The injection nozzle has an oval shape (12 mm long, 1.5 mm wide) so that the oil can be injected over the width of the gears. A PLC control cabinet controls the oil temperature in the oil supply unit as well as the oil injection volume. The injected oil can flow back to the oil supply unit through the two oil drainage holes (Ø24 mm) at the bottom of the two side walls of the test gearbox.

Test gears. As used previously (Refs. 17–19), the well-known test gears

of FZG type C-PT are considered. The geometric data for both the pinion and the wheel are listed in Table 1.

Lubricants. The mineral oils FVA3 and FVA2 (Ref. 16) with viscosity grades of ISO VG 100 and ISO VG32 are considered. Table 2 gives an overview of the main properties of these lubricants.

Operating conditions. The operating conditions were selected based on the empirical equations for the no-load loss introduced in section 1. A set of 12 parameters was chosen. The considered influencing parameters include three circumferential speeds, two oil injection volume rates and two oil injection velocities. The oil temperature is set to 40°C. Table 3 gives an overview on the operating conditions.

Numerical Model

The numerical model is implemented and solved in the commercial CFD software *Ansys Fluent* 18.0.

Governing Equations.

The behavior of fluids can be described with conservation equations (Ref. 12). Based on the Euler equations of motion, the momentum conservation equa-

tions can be extended with mass and energy conservation equations to form a system of partial differential equations of the second order. An overview on the Navier-Stokes equations and turbulence modelling can be found in the previous work of the authors (Ref. 18).

In this study, due to no-load operating conditions, thermal influences are neglected and therefore the energy conservation equation is not considered; a k-ε turbulence model consisting of two coupled transport equations is used. The fluid is considered as Newtonian fluid.

Finite volume method. In order to find an analytical solution for the governing equations, a decoupling of the conservation equations would be necessary. Reynolds or Prandtl numbers were introduced for solving simple problems. For complex applications, no analytical solution can be found and numerical solutions are required. One of the most common methods for practical applications for fluid mechanics is the finite volume (FV) method (Ref. 14). Thereby, the calculation domain is discretized with finite volumes. The accuracy of numerical solutions generally increases with the fineness of the grid and discretization order. In each finite volume, the Lipschitz constancy must be fulfilled.

By integrating the conservation equations on the finite volumes, the divergence term is transformed into a surface integral:

$$\frac{\partial}{\partial t} u(x, t) + \nabla \cdot f(u(x, t)) = 0 \quad (4)$$

$$\int_{\partial \Omega_i} \frac{\partial}{\partial t} u(x, t) d\Omega + \int_{\partial \Omega_i} f(u) \cdot n dS = 0 \quad (5)$$

These surface integrals can easily be determined by Gauss quadrature, so that partial differential equations (in time and space) are converted into a set of linear equations, which can be solved efficiently. The FV method is widely used because of its conservation character.

Volume of fluid method. For oil flow simulations with two media, a two-phase model is necessary. The most common model for immiscible fluids is the Volume of Fluid (VoF) method. It is based on a scalar fraction function C, which is defined as the integral of

Table 1 Geometry of CPT-type gears

	a in mm	z _{1/2}	m _n in mm	α in °	x _{1/2} in mm	b _{1/2} in mm	da _{1/2} in mm
Pinion (1)	91.5	16	4.5	20.0	0.182	14	82.5
Wheel (2)		24			0.171		118.4

Table 2 Properties of the considered mineral oils

Oil	Kinematic viscosity at 40°C, ν(40°C) in mm ² /s	Kinematic viscosity at 100°C, ν(100°C) in mm ² /s	Density at 15°C, ρ (15°C) in kg/m ³
FVA3	95.0	10.7	864
FVA2	32.0	5.4	855

Table 3 Considered operating conditions

Parameter number	Rotational speed of pinion n _i in rpm	Circumferential speed at the pitch circle v _t in m/s	Oil injection volume rate V _{oil} in l/min	Oil injection speed v _{oil} in m/s	Oil
1	130	0.5	2	2.1	FVA3
2					FVA2
3			4	4.2	FVA3
4					FVA2
5	522	2.0	2	2.1	FVA3
6					FVA2
7			4	4.2	FVA3
8					FVA2
9	2166	8.3	2	2.1	FVA3
10					FVA2
11			4	4.2	FVA3
12					FVA2

a fluid's characteristic function in the finite volume (Ref. 15). If a finite volume is "empty" (e.g. 0% oil), the value of C is zero; when the finite volume is "full" (e.g. 100% oil), C equals 1; and when there is a fluid interface in the cell, C is between 0 and 1. The normal direction of the fluid interface is at the position where the value of C changes most rapidly. Each finite volume includes the volume fraction of every fluid (e.g. oil and air), while the fluids share a single set of momentum equations. It means that fluid variables are calculated by the average of the volume fraction of the fluids in the finite volume, whereas the averaged properties are then used to solve a single set of conservation equations in each volume. The resolution of the regarded fluids depends on the size of the finite volumes.

Geometry and mesh. The conservation equations are solved iteratively on finite volumes during calculation. The mesh of the injection-lubricated test gearbox (Fig. 2, right) essentially consists of five domains: the pinion domain; the wheel domain; the outer domain; the oil injection domain; and the remeshing domain. The entire model represents a negative model of the test gearbox. Due to the symmetry of the test gearbox, the simulation model was reduced to one-half by setting the middle plane of the test gearbox to a "symmetry" boundary condition. As the general test gearbox configuration has also been considered by the authors in (Refs. 18–19), some parts are repeated to improve readability.

The mesh of each single domain is connected with the other domains as shown (Fig. 2). The mesh of the pinion and wheel domain is discretized with inflation layers and does not undergo any mesh deformation. During the simulation, the meshes of the pinion and wheel domain rotate inside the gearbox domain at predefined rotational speeds. The outer domain mainly consists of tetrahedral elements and does not undergo any mesh deformation. The elements at the boundary walls of the gearbox are defined as "walls." An oval-shaped oil injection domain is modeled at the position between the injection nozzle and the gear meshing zone. The oil injection volume rate is

defined as an "inlet" by a predefined oil inlet speed at the top of the oval shaped oil injection domain. The oil drainages at the bottom of two sidewalls are defined by two round planes, which are set as the "outflow." The domain of the remeshing zone fills the cavity between the outer domain and the pinion and wheel domain. During operation, the meshing zone of the pinion and wheel is a transient area that changes for every gear meshing position. Thus, the remeshing zone consists of a deformable meshing structure that changes with every time step of the rotating pinion and wheel domain.

The domain of the remeshing zone is discretized with deformable prism elements that deform and stretch with every time step of the rotating pinion and wheel domain. When the mesh quality, e.g. —skewness and orthogonal quality, falls below a predefined minimum mesh quality, the affected elements are reconstructed. This remeshing process is numerically expensive; thus, only the area affected by the rotating and meshing gears is assigned as the remeshing domain. During a numerical analysis, bad element quality and numerical singularities in the very small gap between the tooth flanks, i.e. gear backlash have to be avoided.

Therefore, the very small gap between the tooth flanks is enlarged by scaling the pinion and the wheel to 98% of their actual size. This is currently required for all FV-based CFD simulations of meshing gears. The scaling is not expected to significantly influence the oil distribution and the impulse loss.

For the simulation series, 40 cores of a high-performance computing cluster were used as hardware. A grid with about 0.68 M elements was applied to the mesh model, which results in an average element size between 1.0–1.5 mm³. The time step size was set to 0.1° rotation of pinion. A local convergence criterion of 10⁻⁵ was used for all equations. These settings result in a calculation time of about 8–12 h for a single rotation of the pinion.

A grid sensibility analysis has been performed with different element types. The object of investigation was the no-load loss torque of both gears. In a first step, the half model was discretized with tetrahedral elements. Thereby, the element number was varied from 0.62 M to 1.79 M. In a second step, the half model was mainly discretized with prism elements, which were extruded from a planar area. Thereby, the element number was increased from 0.28 M to 0.71 M. In both cases, the maximum change of the

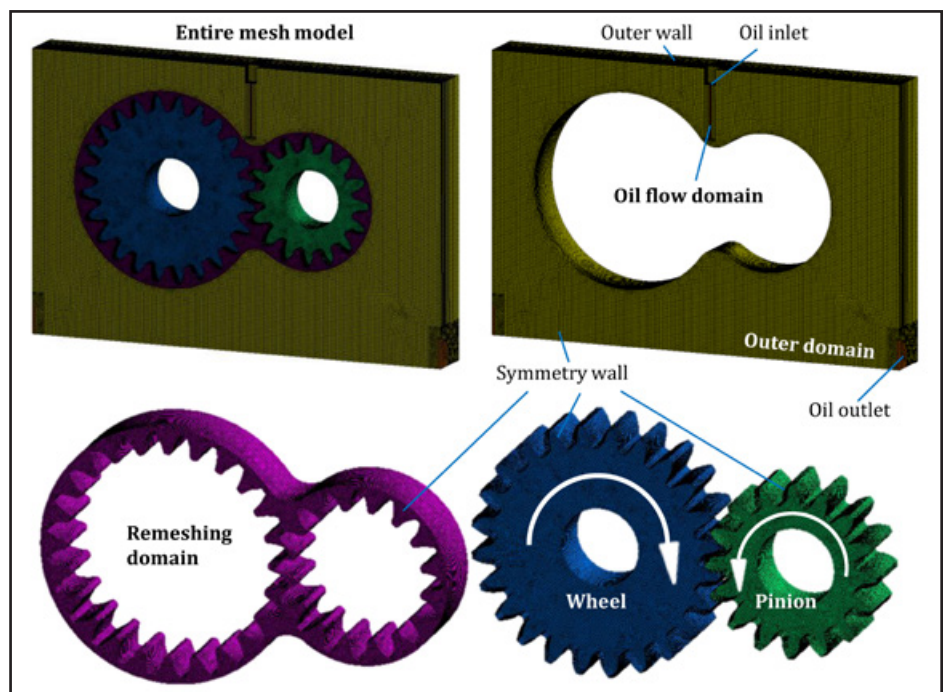


Figure 2 Mesh model of the injection-lubricated test gearbox; entire mesh model (top left); outer domain and oil injection domain (top right); remeshing domain (bottom left); pinion and wheel domain (bottom right).

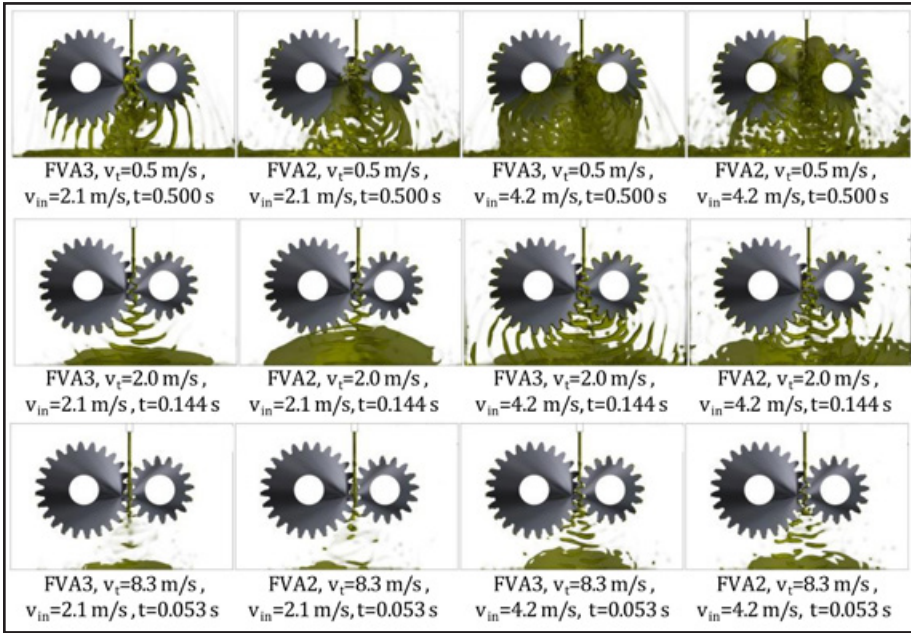


Figure 3 Simulated oil distributions after one rotation of the pinion (front view).

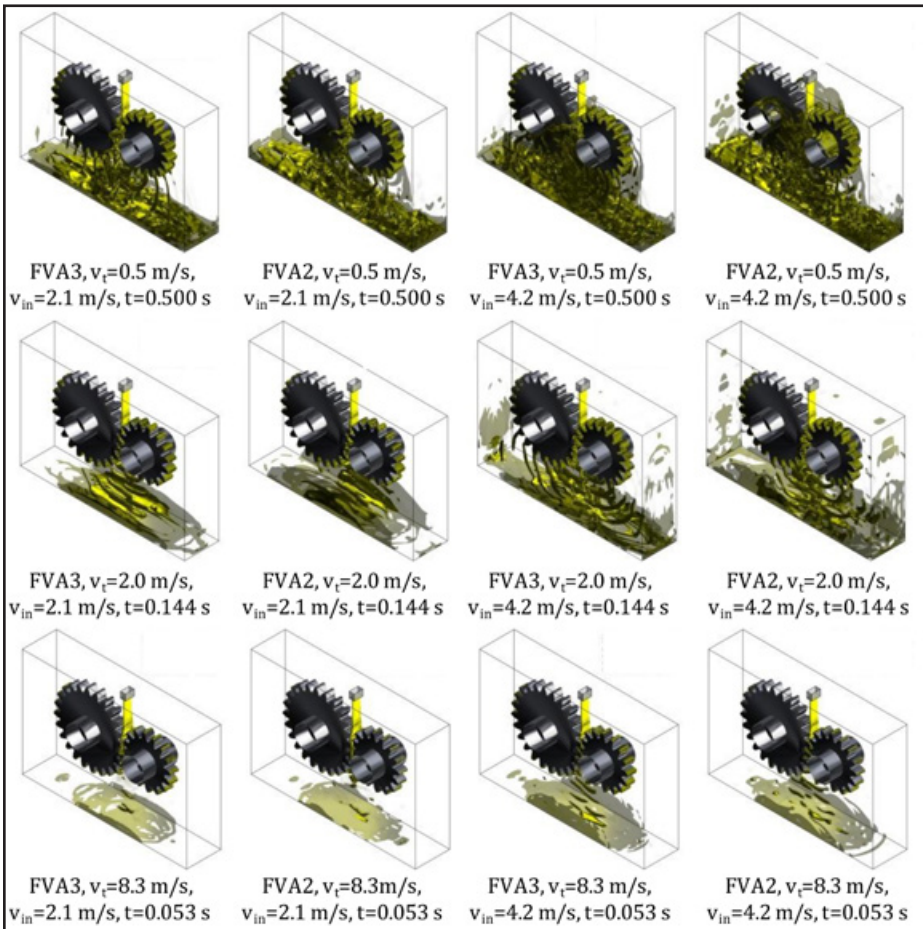


Figure 4 Simulated oil distributions after one rotation of the pinion (isometric view).

no-load loss torque was less than 5%. The oil distribution could be dissolved best with the highest element number. For a similar element number, the computing time of the tetrahedral model was about three times longer than for the prism model. That is mainly due to the higher effort for the remeshing of tetrahedral elements. The tetrahedral model requires stretching and reconstruction of all effected elements in the remeshing zone, whereas for the prism model only the symmetry wall of the remeshing model is stretched and rebuilt. For reasons of computing time, the prism model with 0.68M elements is used.

The no-load loss torque of the gears is derived by the sum of the product of fluid pressure integrated over each finite volume on the circumferential gear surfaces multiplied with the corresponding distance to the axis center. This results in the overall gear no-load loss torque consisting of the impulse, squeezing and windage loss portion.

Results

Results on the oil distribution and the no-load power loss of the injection-lubricated test gearbox are presented based on the operating conditions shown in Table 3.

Oil distribution. Figures 3 and 4 show the simulated oil distributions in front and isometric views, respectively. Thereby, the current oil volume fraction obtained from the CFD simulation is illustrated. All results correspond to a time, when one pinion rotation after the first oil contact has finished. This already results in an almost quasi-stationary oil distribution and loss torque.

The left and right two columns of Figure 3 and Figure 4 correspond to the oil injection speeds v_{in} of 2.1 m/s and 4.2 m/s, respectively, whereas the three rows relate to the circumferential speeds v_t of 0.5 m/s, 2.0 m/s and 8.3 m/s. The influence of the oil injection speed v_{in} and the circumferential speed v_t is superordinate compared to the influence of the oil viscosity (FVA3 and FVA2), which can be observed by comparing the first and second and the third and fourth columns, respectively.

The current oil volume inside the gearbox decreases with increasing

circumferential speed v_t . This is due to the fact that less oil has entered the gearbox after one rotation of the pinion in total. The amount of oil leaving the meshing zone after each gear engagement decreases with increasing v_t due to the shorter cycle time. This and the increase in the centrifugal force with increasing v_t result in more dispersed oil flows with increasing v_t . For $v_t=8.3$ m/s and $v_{in}=2.1$ m/s, the dispersed oil droplets cannot even be resolved properly by the considered mesh size of the CFD model.

When the oil injection speed v_{in} is higher than the circumferential speed v_t , there is a considerable amount of oil dragged in the axial direction and the oil tracks in radial direction after leaving the meshing zone are recognizable. The higher v_{in} compared to v_t , the clearer this observation becomes. For $v_t=0.5$ m/s and $v_{in}=4.2$ m/s, even a damming effect can be observed above the gear meshing zone. The ratio of v_t and v_{in} has a strong effect on the axial and radial squeezing of oil.

In comparison to the circumferential and injection speed, the influence of the oil viscosity (FVA3, FVA2) on the oil distribution is subordinate. For the higher viscous FVA3, pronounced oil tracks gradually swinging off the teeth tend to occur. This is due to the higher resistance to shear stress, which also explains that the oil tracks stick to the gear teeth (cf. $v_t=0.5$ m/s and $v_{in}=2.1$ m/s for FVA2 and FVA3). For the less viscous FVA2, the oil rather appears as small and dispersed oil droplets.

No-load power loss. This section shows the simulation results on the no-load power losses with respect to the results on the oil distribution in the previous section. Each simulated value is averaged over 270° pinion rotation, i.e.—12 gear engagements, and represents the overall gear no-load power loss including the impulse, squeezing and windage portion. The dissolved no-load power loss (not shown) shows maxima when tooth flanks are orientated perpendicular to the injection direction.

Figure 5 shows the CFD simulation results, which are classified into the empirical results according to Mauz (Ref. 21) (cf. Eqs. 2 and 3). The results

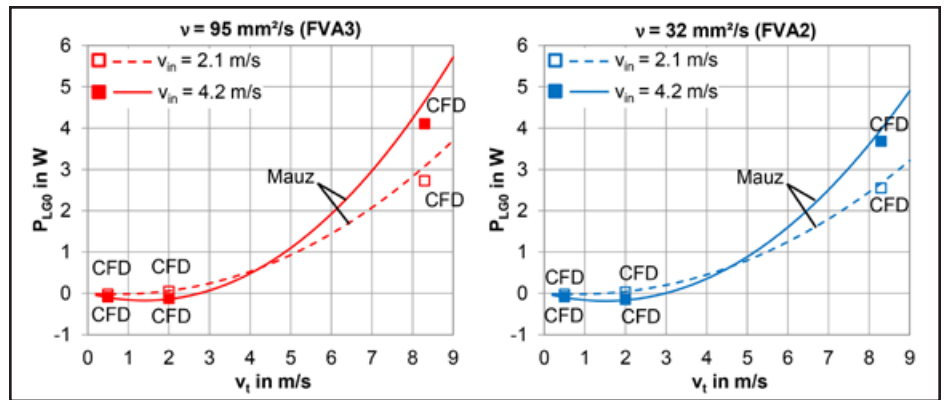


Figure 5 Comparison of no-load power loss between CFD simulation and empirical equations of Mauz (Ref. 21).

are in very good accordance. Note that windage power loss is not explicitly considered in the empirical equations; its portion is considered to be very small for the considered circumferential speeds.

As seen for the oil distribution, the influence of the circumferential speed v_t and the oil injection speed v_{in} is superordinate compared to the influence of the oil viscosity (FVA3 and FVA2). In the following, the results are discussed in groups of the circumferential speeds $v_t=\{0.5, 2.0, 8.3\}$ m/s.

For $v_t=0.5$ m/s, the oil injection speed v_{in} is greater than the circumferential speed v_t . Hence, the oil jet exerts an acceleration torque on the gears, which increases when v_{in} becomes increasingly larger than v_t . This results in a negative no-load power loss, which is however very small.

For $v_t=2.0$ m/s, when the oil injection speed v_{in} almost equals the circumferential speed v_t , the no-load power loss is also very small. When v_{in} is increased to 4.2 m/s, the oil jet again exerts an acceleration torque resulting in a negative no-load power loss.

For $v_t=8.3$ m/s, which clearly exceeds the oil injection speed v_{in} , the injected oil is accelerated to the speed of the tooth flanks, which results in a larger no-load power loss. It rises with v_{in} due to the increasing amount of oil to be accelerated.

In comparison to the circumferential speed v_t and oil injection speed v_{in} , the influence of the oil viscosity is subordinate. This finding is consistent with the empirical equations of Mauz (Ref. 21), as the influence of oil viscosity on the squeezing power loss is relatively small

(Eq. 3) and the impulse power loss is independent of the oil viscosity (Eq. 2).

It should be noted that the no-load power loss caused by injection lubrication is only a small fraction of that created by dip lubrication (Ref. 19).

Conclusion

In this study, a finite volume CFD simulation model of a single-stage injection-lubricated test gearbox was applied to investigate its oil flow and no-load power loss. The results provide physically plausible information on the oil supply and its distribution. The simultaneously simulated no-load losses show very good accordance with empirical equations. It is proved that the CFD method has developed into valuable tools for studying injection-lubricated gearboxes. In the next step, the presented test rig will be adapted for injection lubrication so that the simulation results can be validated by measurement of the no-load loss torque and oil distribution. Future work will focus on the impact of various influencing factors like gear geometry, gearbox housing and high-speed regimes. **PTE**

For more information. Questions or comments regarding this paper? Contact Hua Liu at liu@fzg.mw.tum.de.

References

1. Arisawa, H. "Computational Fluid Dynamics Simulations and Experiments for Reduction of Oil," Kawasaki Heavy Industries. (2014).
2. Arisawa, H., M. Nishimura, H. Imai and T. Goi. "CFD Simulation for Reduction of Oil Churning Loss and Windage Loss on Aeroengine Transmission Gears," ASME Turbo Expo 2009: Power for Land, Sea, and Air, Florida USA, 1, 63–72. DOI=10.1115/GT2009-59226. (2009).
3. Arisawa, H., M. Nishimura, H. Imai and T. Goi. "Computational Fluid Dynamics Simulations and Experiments for Reduction

- of Oil Churning Loss and Windage Loss in Aeroengine Transmission Gears," *J. Eng. Gas Turbines Power* 136, 9, 92604. DOI=10.1115/1.4026952, (2014).
4. Ariura, Y., T. Ueno, Sunaga and S. Sunamoto. "The Lubricant Churning loss in Spur Gear Systems," *Bulletin of the JSME*, Band 16, Nr. 95, 881-892. (1975).
 5. Concli, F. "Numerical Modelling of the Churning Power Losses of Gears: an Innovative 3-D Computational Tool Suitable for Planetary Gearbox Simulation." *Tribology International*, 103, 58-68, DOI=10.13140/RG.2.2.10487.52649. (2016).
 6. Concli, F. "Low-Loss Gears Precision Planetary Gearboxes; Reduction of the Load-Dependent Power Losses and Efficiency Estimation Through a Hybrid Analytical-Numerical Optimization Tool," *Forschung im Ingenieurwesen*, 4, 395-407, DOI=10.1007/s10010-017-0242-0. (2017).
 7. Concli, F. and C. Gorla. "Numerical Modeling of the Power Losses in Geared Transmissions: Windage, Churning and Cavitation Simulations with a New Integrated Approach that Drastically Reduces the Computational Effort," *Tribology International*, 103, 58-68, DOI=10.1016/j.triboint.2016.06.046. (2016).
 8. Concli, F. and C. Gorla. "Windage, Churning and Pocketing Power Losses of Gears; Different Modeling Approaches for Different Goals," *Forschung im Ingenieurwesen*, 3-4, 85-99. DOI=10.1007/s10010-016-0206-9. (2016).
 9. Emmer, K. "Simulation of Oil Flow in Gear Boxes via Smoothed Particle Hydrodynamics," Diplomarbeit, Karl-Franzens-Universität Graz. (2015).
 10. Fondelli, T., A. Andreini, R. Da Soghe, B. Facchini and L. Cipolla. "Numerical Simulation of Oil Jet Lubrication for High-Speed Gears," *International Journal of Aerospace Engineering*, Volume 2015. DOI=10.1155/2015/752457. (2015).
 11. Geiger, J., B.-R. Höhn and K. Michaelis. "Validierung WTplus - Validierung des Programmsystems WTplus 2.0," FVA-Forschungsvorhaben Nr. 69 V, Heft 959, Frankfurt. (2010).
 12. Gersten, K. "Einführung in die Strömungsmechanik" Vieweg, Braunschweig, 1992).
 13. Gorla, C., F. Concli, K. Stahl, B.-R. Höhn, K. Michaelis, H. Schultheiß and J.-P. Stempler. "CFD Simulations of Splash Losses of a Gearbox," *Advances in Tribology*, Volume 2012, DOI=10.1155/2012/616923, (2012).
 14. Hirsch, C. *Numerical Computation of Internal and External Flows*, Elsevier Butterworth-Heinemann, Amsterdam, Heidelberg [u.a.]. (2007).
 15. Hirt, C. and B. Nichols. "Volume of Fluid (VOF) Method for the Dynamics of Free Boundaries," *Journal of Computational Physics* 39, 1, 201-225. DOI=10.1016/0021-9991(81)90145-5. (1981).
 16. Laukotka, E. M. *FVA-Heft Nr. 660 Referenzöle - Datensammlung*, Frankfurt/Main. (2003).
 17. Liu, H., G. Arfaoui, M. Stanic, L. Montigny, T. Jurkschat, T. Lohner and K. Stahl. "Numerical Modeling of Oil Distribution and Churning Gear Power Losses of Gearboxes by Smoothed Particle Hydrodynamics," *Journal of Engineering Tribology*, DOI=10.1177/1350650118760626. (2017).
 18. Liu, H., T. Jurkschat, T. Lohner and K. Stahl. "Determination of Oil Distribution and Churning Power Loss of Gearboxes by Finite Volume CFD Method," *Tribology International*, 109, 346-354, DOI=10.1016/j.triboint.2016.12.042. (2017).
 19. Liu, H., T. Jurkschat, T. Lohner and K. Stahl. "Detailed Investigations on the Oil Flow in Dip-Lubricated Gearboxes by Finite Volume CFD Method," *Journal Lubricants*, presented at 6th World Tribology Congress 17.-22, September, Beijing, China, DOI=10.3390/lubricants6020047. (2018).
 20. Massini, D., T. Fondelli, B. Facchini, L. Tarchi and F. Leonardi. "High-Speed Visualizations of Oil Jet Lubrication for Aero-Engine Gearboxes," *Energy Procedia*, 101, 1248-1255. DOI=10.1016/j.egypro.2016.11.140. (2016).
 21. Mauz, W. "Hydraulische Verluste von Stirnradgetrieben bei Umfangsgeschwindigkeiten bis 60 m/s," Dissertation, Universität Stuttgart. (1987).
 22. Mizutani, H., Y. Isikawa and D.P. Townsend. "Effects of Lubrication on the Performance of High-Speed Spur Gears," *Fifth International Power Transmission and Gearing Conference, Chicago, USA*. (1989).
 23. Monaghan, J. J. "Smoothed Particle Hydrodynamics," *Rep. Rog. Phys.*, 68, DOI=10.1088/0034-4885/68/8/R01. (2005).

For Related Articles Search

lubrication

at www.powertransmission.com

Hua Liu studied Mechanical Engineering and Automotive Technology with a focus on numerical mechanics and drive engineering at the Technical University of Munich (TUM). During his Master's program he did research in the area of finite element analysis of plastic gears. After he had finished his Master's degree in 2014, he has worked as a research associate at FZG focusing on the application of CFD methods in gearboxes.



Felix Link studied Mechanical Engineering and Automotive Technology with a focus on computer-aided engineering at the Technical University of Munich (TUM). During his Master's program he did research in the area of the application of CFD methods in gearboxes. After finishing his Master's degree in 2018, he has worked as an engineer for structural mechanics in aircraft engines.



Thomas Lohner studied Mechanical Engineering and joined the Gear Research Centre (FZG) at the Technical University of Munich (TUM) as a research associate in 2012. After finishing his Dr.-Ing. degree in 2016, he has worked as post-doctoral fellow and is head of the department EHL-Tribological-Contact and Efficiency at FZG. Lohner's research interests include machine elements, gears and power transmission systems, as well as tribology, elasto-hydrodynamic lubrication, efficiency and heat management.



Karsten Stahl studied Mechanical Engineering at the Technical University of Munich. Afterwards, he joined the Gear Research Centre (FZG) at the Technical University of Munich (TUM) as research associate and finished his Dr.-Ing. degree in 2001.



The same year he started as gear development engineer at the BMW group in Dingolfing, subsequently becoming head of the prototyping, gear technology and methods group in 2003. In 2006 he moved to the BMW/MINI plant in Oxford, UK, and the next year (2007) he became department leader for validation driving dynamics and powertrain. In 2009 he returned to Munich as manager for pre-development and innovation management within BMW driving dynamics and powertrain in Munich. Since 2011, Karsten Stahl is a full professor at the Institute for Machine Elements and head of the Gear Research Centre at the Technical University of Munich. The FZG employs about 80 associates — 50 of them PhD candidates and more than 200 students. Organized in 5 departments, Prof. Stahl's research focuses on experimental and theoretical investigations of endurance, tribology, NVH, materials and fatigue analysis. Components in the focus are cylindrical, bevel, hypoid and worm gears, clutches, synchronizers rolling-element bearings, and drive systems."